Effects of Toe Grouting on Axial Performance of Drilled Shafts Socket in Intermediate Geomaterial

San-Shyan Lin[1], Yen-Liang Yin[2], Kuo-Chen Fu[3], Yung-Kuang Lin[4], Chin-Jung Kuo[5], Yu-Heng Chang[6]
[1]*Depart of Harbor and River Eng., National Taiwan Ocean University*
[2,3]*Nan Shan Life Insurance Co., Ltd.*
[4,5]*Mice Engineering Consultants Co.,Ltd.*
[6]*Diagnostic Engineering Consultants Co., Ltd.*
E-mail: sslin46@gmail.com

ABSTRACT: In this paper, the axial performance of two heavily instrumented drilled shafts, with and without toe grouting, socket in intermediate geomaterials in Taipei are evaluated based on the results of pile load tests. The load versus settlement at pile head and the t-z curves along shaft, especially for the part socket into intermediate geomaterials, are main concerns. The t-z curves interpreted from the measured data along shaft are also simulated by the hyperbolic model. The value of friction factor (β) of the shaft with or without grouting is also compared in the paper. It's found toe grouting improved not only the end bearing capacity but also the frictional resistance of the tested shaft.

KEYWORDS: Pile load test, Intermediate geomaterial, Drilled shaft, Hyperbolic model

1. INTRODUCTION

Performance of drilled shaft foundation is strongly dependent upon the local geological condition. Hence, the load-settlement test of drilled shaft foundation is often performed to refine the design assumptions for geomaterial and pile characteristics and interaction between pile and geomaterial. A forty five stories high rise building project located next to the highest building in Taiwan, Taipei 101, is planned and is under designing. Use of rock or intermediate geomaterial (IGM) socket drilled shafts has been increased in the past decade in Taiwan. How to estimate side friction resistance of shaft through rock layer or IGM has been major concerns of the local geotechnical engineers. In addition, effect of toe grouting on skin frictional resistance through rock or IGM layer is another concern. Effects of toe grouting on bearing capacity improvement of drilled shafts socket in rock or in gravel layer can refer to Lin et al. (2000, 2008 and 2010).

To compare the axial performance of drilled shafts through IGM layer, two compressive tests were proposed before designing of these shafts. Both shafts, with diameter of 1.5m, were heavily instrumented with strain gages. The two compressive loading tested shafts, C1 and C2, were 66.5m long (without toe grouting) and 58.3 m long (with toe grouting), respectively. IGM socket length of the former and the latter shafts were 20m and 13m, respectively. Performance of the tested shafts was evaluated based on the loading test results. In addition, static load test up to 75MN conducted on drilled shaft set the record as the highest load ever tested for a single drilled shaft in Taiwan. Effect of the toe grouting was also evaluated by comparing the performance between C1 and C2 shafts. The t-z curves of the frictional resistance of both shafts were also studied and characterized using hyperbolic model. The values of friction factor (β) of the tested shafts were also compared in the paper.

2. SUBSURFACE CONDITIONS

The standard penetration test and ground investigation were carried out at center of each test shaft to explore the subsurface conditions along depth. The typical physical properties and strengths of subsurface soil are presented in Table 1 and Figure 1, respectively. The vertical axis of Fig. 1 is elevation while the number given by the logging is depth. The unconfined compressive strength of the rock layer below the soil layer is listed in Table 2. Since the unconfined compressive strength of the rock are only between 0.46 and 3.76 MPa, it is classified as IGM based on the suggestion of Hassan et al. (1997). The pullout test of T1, tested at the same site, is not discussed in the paper. In general, the subsurface condition at the shaft testing site was found to be characterized by a 45m thick clay layer that lies beneath the backfill surface layer. Alternating sandstone and shale rock layers were encountered below the clay layer. Relatively low SPT-N values were observed from ground surface down to about 30m deep. Since the cut-off level of the shaft at GL -23.75 and the low SPT-N value of the clay layer, the frictional resistance of the shaft embedded in the IGM layer was the main concern of this project.

Table 1 Physical properties and strength of the soil strata

Shaft	Layer	Depth (m)	Classification	SPT N	γ_r (kN/m^3)	W_n (%)	e	S_u (kN/m^2)	$\bar{\phi}$ *(deg.)*
C1	1	0~-1.8	SF/CF	2~>50	18.74	32.4	0.89		28
	2	-1.8~-29.7	CL	~9	15.60~20.31	23~81	0.58~1.99	19.62~57.88	22.7~24.5
	3	-29.7~-46.1	CL	5~50	15.40~21.29	16~59	0.42~1.56	81.42~110.85	30
C2	1	0~-0.4	SF/CF	2~>50	18.74	32.4	0.89		28
	2	-0.4~-34.6	CL	~9	15.60~20.31	23~81	0.58~1.99	19.62~57.88	22.7~24.5
	3	-34.6~-45.3	CL	5~50	15.40~21.29	16~59	0.42~1.56	81.42~110.85	30

γ_r : unit weight ; W_n : water content ; e : void rati

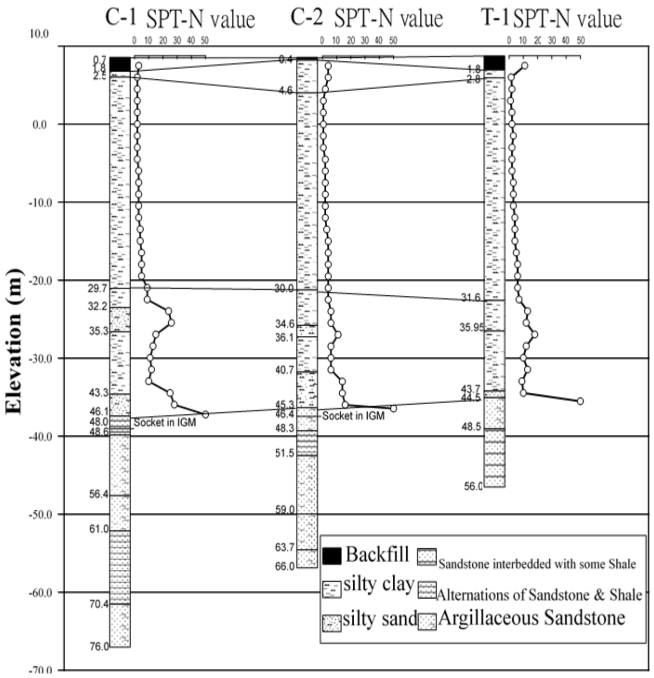

Figure 1 SPT-N Value in Soil and IGM

Table 2 Unconfined Compressive Sstrength of IGM Layers

Shaft	Ground Level (m)	unconfined compressive strength (MPa)
C1	-47.30~-47.45	1.42
	-48.25~-48.40	1.71
	-52.05~-52.20	1.25
	-55.55~-55.70	2.16
	-59.05~-59.20	2.85
C2	-50.80~-50.95	3.76
	-54.60~-54.75	0.56
	-56.85~-57.00	0.46
	-58.45~-58.60	1.3
	-62.70~-62.95	3.39
	-63.40~-63.55	2.17

3. DRILLED SHAFTS CONSTRUCTION AND TESTING SETUP

The reverse circulation was used for shaft installation. Excavation was conducted via tri-blade auger. Drilling was also done with a polymer slurry pumped into a shaft bore hole. The tremie method was used for shaft concreting, using a slump between 18 and 22cm. Four 5.08cm PVC piles were attached to the rebar cage on each shaft for sonic logging integrity testing. Good concrete quality was observed for both test shafts after the integrity testing.

To evaluate the total load carried at different depths along the shaft, rebar gauges were installed at pre-selected depths of each shaft. The selected levels of C1 shaft were 1.5, 23.75, 32.2, 35.3, 43.3, 46.1, 48.6, 54.2, 56.4, 58.7, 61, 62.5, 64, and 65.5m deep below ground level. For the C2 shaft, the selected levels were 1.5, 13, 23.75, 34.6, 40.7, 45.3, 51.5, 53.2, 54.7, 56.2, and 57.m below ground surface. The gauges were attached to the rebar cage in sets of four at each depth. Given modulus of pile section, load distribution along the pile shaft can be assessed assuming same axial strain is developed in concrete and steel. Since the cut-off level is 23.75m below ground surface, both C1 and C2 were also installed with rod extensometers at level of 23.75m plus additional level of 65.5m and 57.5m, respectively.

Pile toe grouting was conducted using the so called modified U-shape pipe for shaft C2 (Lin et al., 2000). A high-pressure water jet was used to clean undesirable material from the shaft base via the drilling rod. The water circulated at least twice to and through the defective zone of the shaft. Once the returning water was clean for a given amount of time, washing was stopped. After cleaning of the base sediment had been completed, the grout, at a pressure of 4,900 kPa, injected through one of the base grouting holes. Detail information on the toe grouting can refer to Lin et al. 2000.

Location of the tested shafts C1and C2 is given in Figure 2. Photo of the test shaft C1 is also shown in Figure 3, in which BH represents bore hole. The quick test procedure of ASTM D1143 was followed for compressive tests.

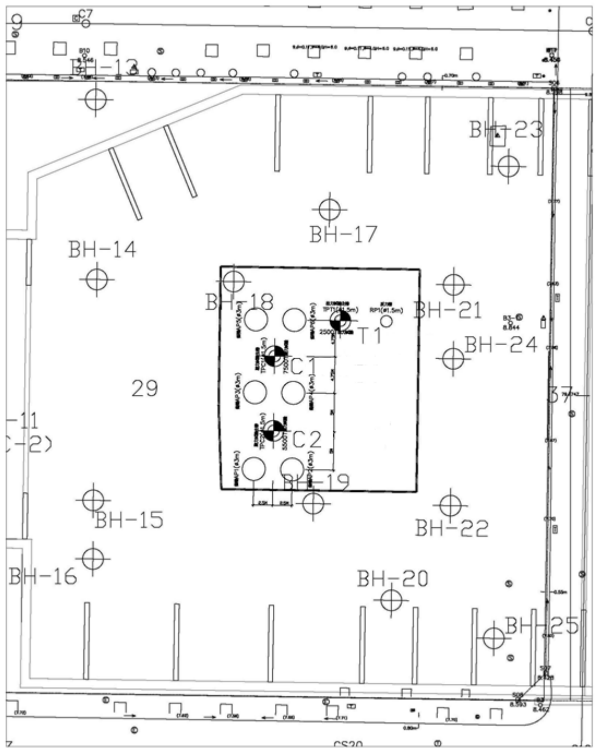

Figure 2 Location of C1 and C2 Shafts in the project

4. TEST RESULTS AND DISCUSSION

The load versus settlement relations at pile head of both shafts are presented in Figure 4. As shown in the figure, the loads versus displacement relationships of both tested shafts are almost identical up to 40 MN. Slightly higher capacity was observed on C2 shaft when the applied load was between 40MN and 50MN, although C2 shaft was shorter. It is believed the total capacity of the shaft C2 was improved by toe grouting. When the maximum applied loading of C1 shaft reached 75MN, the corresponding displacement increased up to 143.96mm at the head and 90.52mm at the toe. For C2 shaft, the displacement, under maximum applied loading 55MN, reached 67.57mm at the pile head and 26.18mm at the pile toe. Unit end bearing resistance versus toe displacement relation was nearly linear as observed from C1 shaft shown in Figure 5. Higher end bearing resistance of C2 was also observed due to toe grouting improvement. Under the same displacement, the end bearing resistance of C2 was 3.5 times higher than that of C1.

The axial load transfer along depth of C1 and C2 is given in Figure 6 for comparison. Each shaft appeared to have different load distribution rate. Under the same applied load at head, smaller end bearing resistance was mobilized on C2 shaft when compared to that of C1 shaft.

Figure 3 Photo of test C1 Shaft

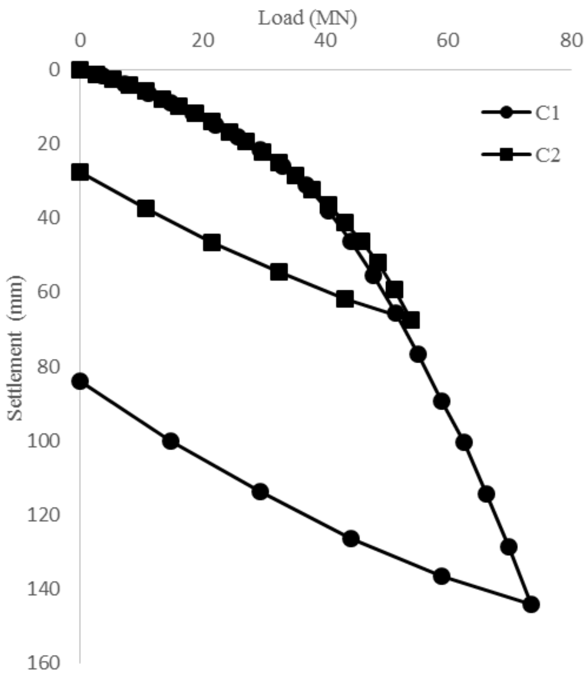

Figure 4 Pile head movement of the tests shafts C1 and C2

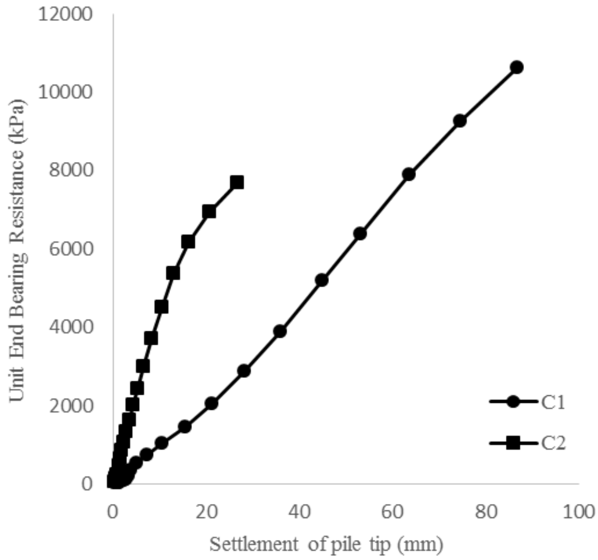

Figure 5 mobilized unit bearing versus settlement relationship of the Shafts C1 and C2

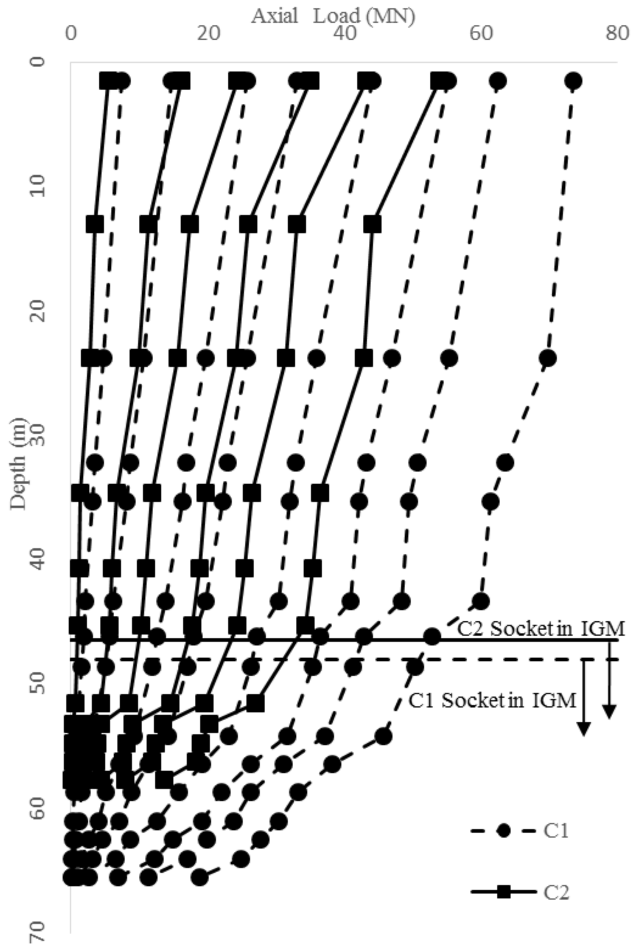

Figure 6 Load distribution of tested shafts C1 and C2

The t-z curves of the clay layer and the IGM layer at various elevation are given in Figures 7(a) and 7(b), respectively. As shown in Figure 7(a), softening behavior for C1 at GL-35.3~-43.3m was observed. All t-z curves for C2 stayed hardening behavior. Embedded in IGM layer, higher side frictional resistance of C2 was also observed as given in Figure 7(b). Again, better performance of C2 shaft is attributed to toe grouting. For the ground level between -56m and -58m, the frictional resistance of both shafts showed lower resistance than that of the top layer. It is believed that there exists a lower strength rock layer sandwiched between two stronger layers, as compared to the information given in Table 2.

5. HYPERBOLIC MODEL

In order to simulate the axial side frictional resistance and the axial displacement relationships at different elevations of the test shafts, the hyperbolic model, used by Gupta (2012), is adopted in this paper. The hyperbolic function can be expressed as (Gupta 2012)

$$f_s = \frac{(\Delta/d)}{\frac{1}{G_i} + \frac{(\Delta/d)R_f}{f_{su}}} \quad (1)$$

where f_s= side frictional resistance developed at any instant of time when the displacement of the drilled shaft embedded in soil or IGM at the depth of interest is Δ, d = diameter of the drilled shaft, f_{su}= ultimate side frictional resistance that could be reached before the asymptotic value, R_f= failure factor and G_i= initial shear modulus.

Similar hyperbolic form has also been successfully used by Lin (1997) to simulate the t-z curves of the pile along depth. Using transformed axes (Desai and Christian 1979), the hyperbolic model of Eq. (1) becomes linear when the ordinate equal to $1/G_i$ and the slope of the line as $1/f_{su}$.

The length of the test shaft was subdivided into segments. G_i and f_{su} values determined from Δ/d versus f_s curves obtained from load tests are listed in Table 3. The simulated and the measured results for C1 and C2 at clay layer is obtained as shown in Figures 8(a) to 8(b), respectively. Due to the property of the hyperbolic function, the softening behavior cannot be captured by the model. Better agreement was obtained between the simulated and the measured results of rock layer as given in Figure 9. Table 3 also shows the β factor calculated as ratio f_{su}/σ_0 . β for IGM suggested by O'Neill and Reese (1999) is expressed by the following

$$\beta = 2.1261z^{-0.2965} \quad (2)$$

where z= depth in meter. The β values estimated by the hyperbolic model and by the equation (2) along depth of shaft C1 and shaft C2 was also compared in Figure 10. The trend of of the Eq. (2) is different from the estimated values of the hyperbolic model.

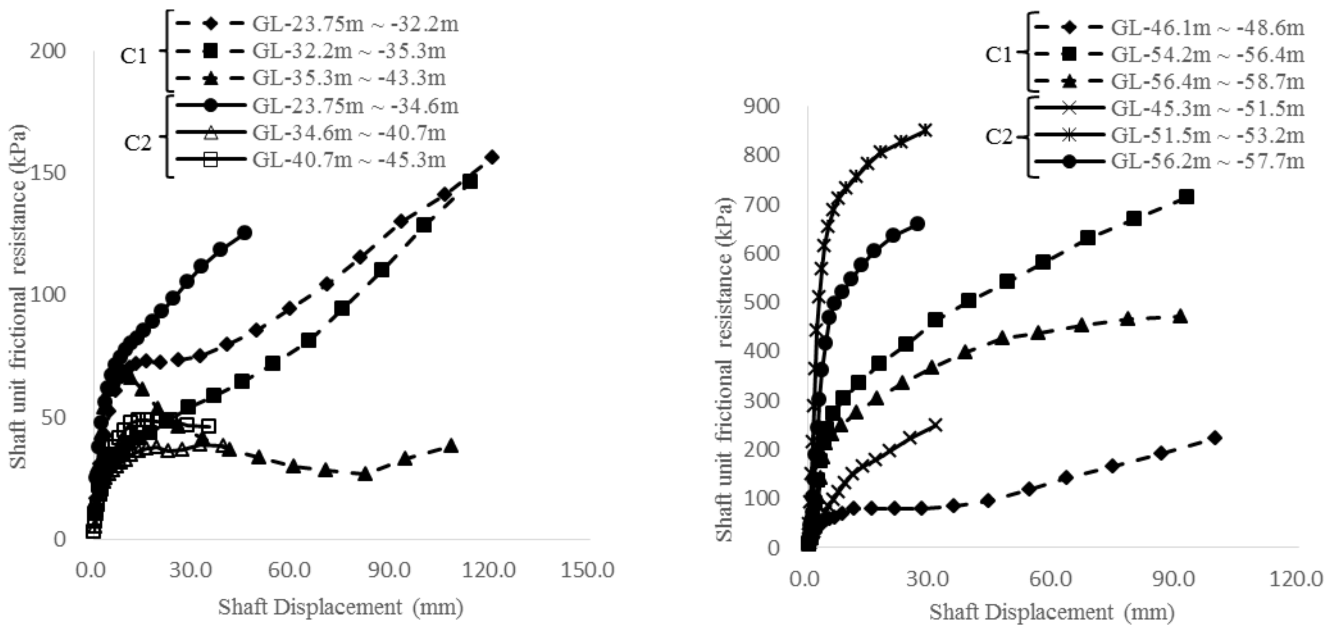

(a) Clay layer (b) IGM layer

Figure 7 Shaft unit frictional resistance versus displacement of shafts C1 and C2

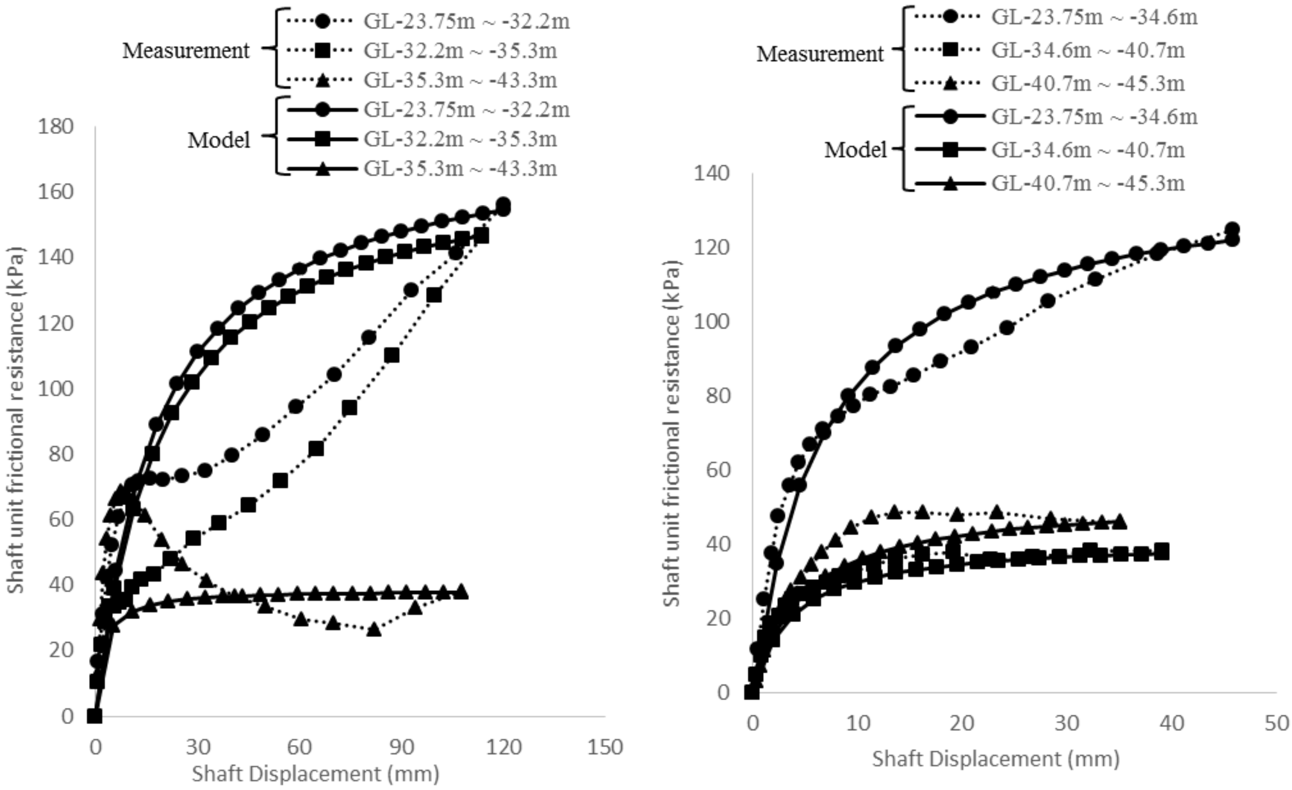

(a) C1 shaft

(b) C2 shaft

Figure 8 Hyperbolic model fitting of t-z curves in clay layer

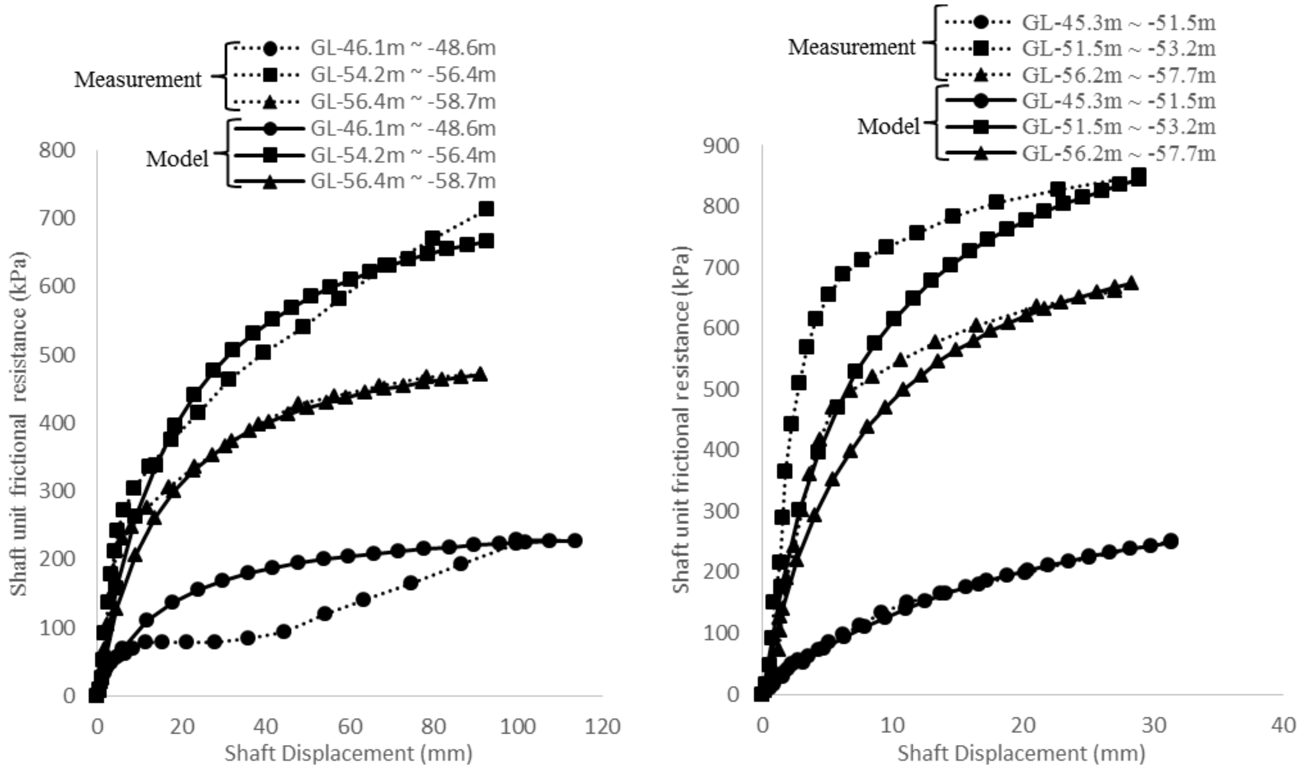

(a) C1 shaft

(b) C2 shaft

Figure 9 Hyperbolic model fitting of t-z curves in IGM layer

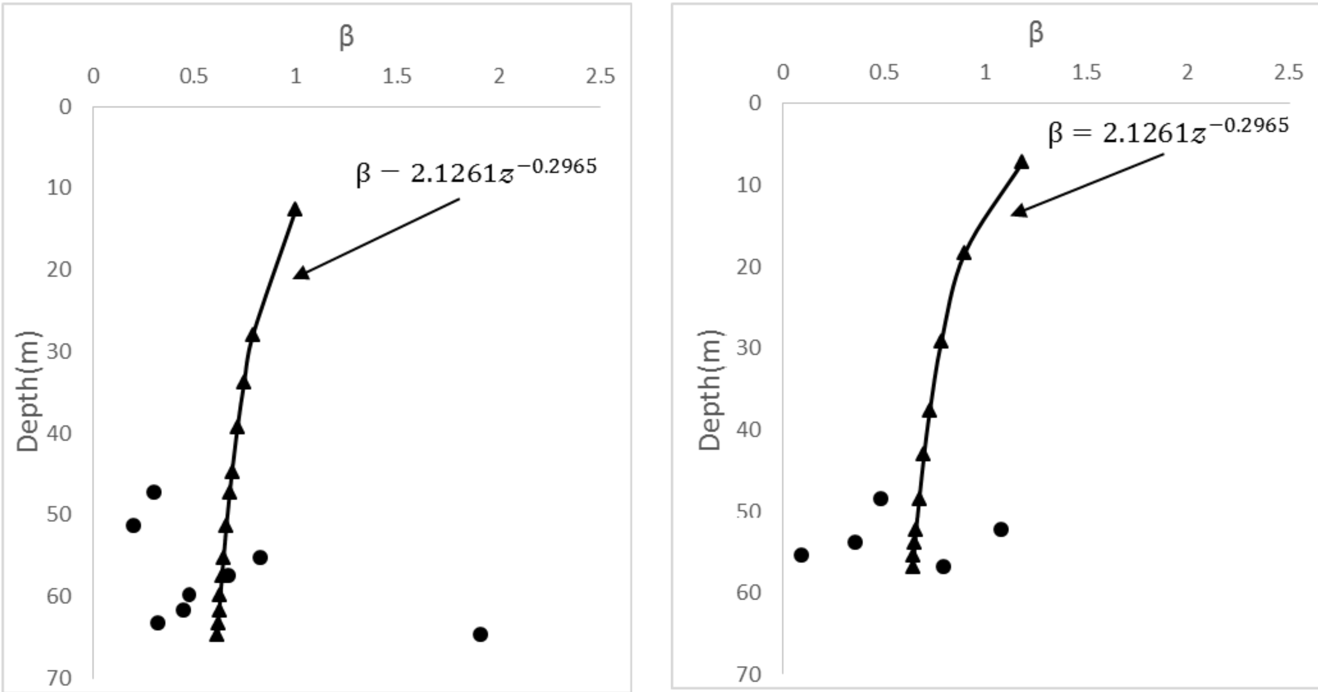

(a) C1 shaft (b) C2 shaft

Figure 10 β factors determined from load test

Table 3 G_i and f_{su} values determined from Δ/d versus fs curves

Ground Layer	Shaft	Mid-depth (m)	G_i (kN/m^2)	f_{su} (kN/m^2)	*β*
Clay Layer	C1	-27.975	14765	177.66	-
		-33.75	13159	172.15	-
		-39.3	26541	38.52	-
	C2	-29.175	30413	140.53	-
		-37.65	16417	41.20	-
		-43	16709	52.51	-
IGM Layer	C1	-47.35	28720	260.50	0.00907
		-55.3	62951	869.71	0.013816
		-57.55	54427	549.60	0.010098
	C2	-48.4	28337	429.27	0.015149
		-52.35	219000	1055.00	0.004817
		-56.95	164630	860.68	0.005228

6. CONCLUSIONS

Axial pile load tests on performance of two drilled shafts socket in IGM were carried out at a high rise building project in Taipei. Based on the results of pile load test discussed in this paper, the following conclusions are drawn:

(1) Toe grouting improved not only the end bearing capacity but also the frictional resistance of the tested shaft C2.

(2) The hyperbolic model provided a good fit with Δ/d versus f_s relationship with hardening behavior obtained from load tests on instrumented shafts. Fitting the initial and the residual part of the Δ/d versus f_s relationship, the hyperbolic model could also reasonably simulate the softening behavior obtained from the measured data. In addition, the model used for the pile load test data also provided reasonable estimate of G_i, f_{su} and β values.

(3) The β values estimated in the paper did not follow the trend suggested by O'Neill and Reese (1999), because of the alternating layered property of the IGM.

(4) Static load test up to 75MN conducted on drilled shaft set the record as the highest load ever tested for a single drilled shaft in Taiwan.

7. ACKNOWLEDGEMENT

The presented study was carried out as part of a research project funded by the Ministry of Science and Technology of Taiwan, ROC (NSC 102-2221-E-019 -028 -MY3). The first author is grateful for the financial support.

8. REFERENCES

American Society for Testing and Material (1994) "Standard test methods for deep foundations under static axial compressive load", ASTM D1143, USA.

Desai, C.S., and Christian, J.T. (1977) *Numerical Methods in Geotechnical Engineering*, McGraw Hill, New York, USA.

Gupta, R.C. (2012) "Hyperbolic Model for Load Tests on Instrumented Drilled Shafts in Intermediate Geomaterials and Rock" Journal of Geotechnical and Geoenvironmental Engineering, 138(11), 1407-1414.

Hassan, K.M., O'Neill, M.W., Sheikh, S.A., and Ealy, C.D. (1997) "Design Method for Drilled Shafts in Soft Argillaceous Rock", *Journal of Geotechnical and Geoenvironmental Engineering*, ASCE, 123(3), 272-280.

Lin, S.S., Liao, J.C., Wang, K.J., and Lin, Y.K. (2010) "Load Capacity of Drilled Shafts Socketed in Andesite Rock" in *The Art of Foundation Engineering Practice*, GSP No. 198, ASCE, 359-370.

Lin, S.S., Liao, J.C., Wang, K.J., and Chang, Y.H. (2008) "Effects of Tip Grouting on Capacity of Shafts Socket in Gravel Layer" *Geotechnical Engineering Journal*, 39(1), 13-18.

Lin, S.S., Lin, T., and Chang, L.T. (2000) "A Case Study for Drilled Shafts Base Mud Treatment", in *New Technological and Design Developments in Deep Foundations*, GSP No. 100, ASCE, pp. 46-58.

Lin, S.S. (1997) "Use of Filamented Beam Elements for Bored Pile Analysis", *Journal of Structural Engineering*, ASCE, 123(9), pp. 1236-1244.

O'Neill, M.W., and Reese, L.C. (1999) *Drilled Shafts: Construction Procedures and Design Methods*, Rep. FHWA-IF-99-025, Federal Highway Administration, Washington D.C., USA.